

Table I. RR Frequencies and Shifts (cm^{-1}) for MTPP Triplets and Radical Cations and Anions

assignment	ZnTPP	$\Delta^*{}^a$	$\Delta^+{}^b$	$\Delta^-{}^c$	MgTPP	$\Delta^*{}^a$	$\Delta^+{}^b$	$\Delta^-{}^c$	PdTPP	Δ^*
A ^d phenyl ^e	1600	-2	-2	-1	1602		-2		1595	-2
ν_2 C _b C _b	1549	-3	-7	+3	1550	-4	-11	+5	1557	-7
ν_{12} C _b C _b	1494	-4	-19	+2	1496	-3	-9	+3		
ν_4 C _a N	1355	-3	-12	-6	1353	0	-20	+4	1364	-1
C C _m Ph	1244	-5	0	-6	1239	-3	0	-4	1235	-1
ν_5 δ C _b H	1081	-5	+8	-15	1080	-5	-22	-9	1080	-3
E phenyl	1038				1033					
F phenyl	1005	-4	0	-2	1005	-2	0	-1	1013	0
ν_6 C _a C _m	1005	-4	-22	-18	1005		-20	-13		

^a Δ^i frequency shift relative to MTPP for MTPP⁺, MTPP⁻, MTPP* ($i = +, -, *$). ^b From ref 5a. ^c From ref 5b. ^d Mode labels from ref 6a. ^e Principal internal coordinate contributor to the mode, from ref 6b.

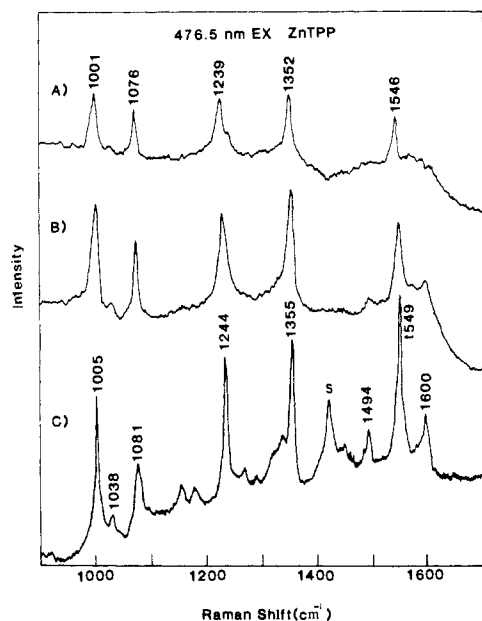


Figure 1. (A) Difference spectrum, (B) - (C), attributed to ZnTPP*. (B) Stationary sample in a NMR tube, excited at 135 °C with a 476.5-nm Ar⁺ laser beam (250 mW, focused); the sample was cooled in a cold N₂ stream. The spectrum is the sum of five scans, each of a fresh sample from which O₂ was removed by freeze pumping and recorded with a computer-controlled Spex 1401 scanning monochromator, with a cooled photomultiplier tube and photon-counting electronics; 0.5 cm^{-1}/s scan rate, 1-s time constant, 5- cm^{-1} slit width. (C) As in (B), but the NMR tube was spun, and the laser power was lowered to 30 mW; seven scans were added.

Table I. The middle spectrum was obtained in the same cell, but without spinning, and with increased laser power (250 mW). There are clear broadenings and shifts in the ZnTPP RR bands, and the solvent band at 1421 cm^{-1} is greatly diminished in relative intensity. We interpret these effects as due to pumping of the ground state to form the ZnTPP triplet state (via the excited singlet), the Raman spectrum of which is elicited by a second laser photon. Because the quantum yield for triplet formation is high (0.8) and the triplet lifetime is long (1.3 ms),⁷ pumping is effective even with the relatively low-power CW laser excitation. Moreover, the excitation wavelength is in resonance with the strong triplet absorption (470 nm, $\epsilon \sim 71\,000\ \text{M}^{-1}\ \text{cm}^{-1}$).⁸ The disappearance of the solvent band is due to the triplet-triplet absorption at this wavelength and is strong evidence for triplet formation in relatively large abundance (which, however, has not been quantitated). The Soret band of the ground state is at higher energy ($\epsilon = 2.5 \times 10^5$ at 416 nm) but is close enough to provide both resonance enhancement of the ground state and sufficient absorption ($\epsilon \cong 4600$ at 476.5 nm) for pumping. The top spectrum of Figure 1 is that

of the triplet state, obtained by subtracting the bottom spectrum (ground state) from the middle spectrum (mixture); the weighting factor was gradually increased to the point where negative peaks began to be seen due to oversubtraction. Similar spectra are observed for MgTPP and PdTPP, with excitation at 488.0 and 457.9 nm, respectively, for resonance with the triplet absorption bands, 485 nm ($\epsilon \sim 72\,000$) for MgTPP, and 450 nm ($\epsilon \sim 47\,000$) for PdTPP.⁸ Triplet quantum yields (0.8 and 1.0) and lifetimes (1.3 and 0.4 ms) are likewise suitably large for MgTPP and PdTPP.⁷

The porphyrin skeletal mode frequencies are all slightly lower for the triplet than for the ground states. Table I lists the triplet down shifts, 1–7 cm^{-1} , along with the shifts observed for the radical cations^{5a} and anions^{5b} of MgTPP and ZnTPP reported by Itoh and co-workers. Since the triplet excited states are formed by promoting an electron from the highest filled orbital to the lowest unoccupied orbital, the structural effects might be expected to be a superposition of those observed for radical cation and radical anion formation. Indeed, the opposing vibrational shifts which tend to be seen for electron addition and removal (Table I) help to explain the very small shifts seen for the triplet states. For example, the triplet shift for the 1550- cm^{-1} mode, -3 and -4 cm^{-1} for ZnTPP and MgTPP, is close to the resultant of the cation and anion shifts (-7 + 3 = -4; -11 + 5 = -6). For other modes, the resultant deviates more widely from the observed triplet shift. All of these shifts are relatively small; however, and it is not surprising that the simple superposition approximation would fail to account for their details.

A particularly interesting question is the fate of the phenyl modes, several of which have been identified in ground-state RR spectra of TPP's.^{6b} Although relatively weak, they are clearly resonance-enhanced, although the phenyl substituents are known to be oriented at nearly right angles to the porphyrin ring,⁹ and conjugation is not significant in the ground state.¹⁰ It was suggested^{6b} that resonance enhancement reflected an increase in conjugation in the excited state. If conjugation were increased in the excited state, one might expect the phenyl mode frequencies to decrease appreciably. The clearest phenyl mode in the ground-state spectra is the one at $\sim 1600\ \text{cm}^{-1}$. No distinct band is seen in the triplet spectra, but in each case there seems to be a broad underlying envelope near this frequency (see Figure 1). While this envelope could have a number of explanations, an interesting possibility is that it reflects an inhomogeneous distribution of phenyl orientations with a broad range of vibrational frequencies. Such a distribution has a plausible physical basis, since the driving force for phenyl rotation into the porphyrin plane which is provided by the electronic excitation (the e_g orbital has particularly large coefficients at the meso carbon atoms⁴) encounters steric resistance from the nonbonded interactions between the protons at the ortho positions of the phenyl groups and those on the outer pyrrole carbon atoms.⁹ Consequently the phenyl torsion potential in the excited state may be relatively flat. Nevertheless, the vibrational frequencies are expected to be sensitive to the torsion angle for orientations close to coplanar

(6) (a) Stein, P.; Ulman, A.; Spiro, T. G. *J. Phys. Chem.* **1984**, *88*, 369–374. (b) Burke, J. M.; Kincaid, J. R.; Spiro, T. G. *J. Am. Chem. Soc.* **1978**, *100*, 6077.

(7) Darwent, J. R.; Douglas, P.; Harriman, A.; Porter, G.; Richoux, M.-C. *Coord. Chem. Rev.* **1982**, *44*, 83.

(8) Harriman, A. *J. Chem. Soc., Faraday Trans. 2* **1981**, *77*, 1281.

(9) Eaton, S. S.; Eaton, G. R. *J. Am. Chem. Soc.* **1975**, *97*, 3660.

(10) LaMar, G. N.; Eaton, G. R.; Holm, R. H.; Walker, F. A. *J. Am. Chem. Soc.* **1973**, *95*, 63.

because of the effect of conjugation. It is notable that the bandwidths for the skeletal modes are somewhat larger in the triplet than in the ground state spectra (~ 15 vs. 12 cm^{-1} FWHM). The skeletal mode frequencies are expected to be less sensitive to phenyl conjugation because the electronic influence is spread over a larger ring, but their increased width may nevertheless be a reflection of the proposed inhomogeneous distribution.

Acknowledgment. This work was supported by Grant DE-AC02-81ER10861 from the US Department of Energy.

Registry No. MgTPP, 14640-21-2; ZnTPP, 14074-80-7; PdTPP, 14187-13-4.

Laser-Induced Excited-State Ligation Changes for Nickel Tetraphenylporphyrine Monitored by Raman Spectroscopy

Dongho Kim and Thomas G. Spiro*

Department of Chemistry, Princeton University
Princeton, New Jersey 08544

Received December 6, 1985

Metalloporphyrins offer the interesting possibility of undergoing changes in axial ligation associated with the pumping of excited ligand field states via intersystem crossing from initially populated porphyrin $\pi-\pi^*$ states.^{1,2} One example is the extremely rapid³ and efficient photodissociation of the CO adduct of heme proteins, which has been widely exploited in studying the heme-linked protein dynamics of these O_2 -carrying and -activating macromolecules.⁴ Nickel porphyrins offer an attractive system for investigation since they are 4-coordinate and low spin in noncoordinating and weakly coordinating solvents but 6-coordinate and high spin in strongly coordinating solvents.⁵ Holten and co-workers have shown with transient optical spectroscopy that the accessible excited state (low spin) of the 6-coordinate species rapidly loses its axial ligands, while the excited state of 4-coordinate nickel porphyrin (high spin) becomes ligated, thanks to the hole created in the d_{z^2} orbital. It should therefore be possible to shift the equilibrium between 4- and 6-coordinate species with photons. In this report we demonstrate such pumping with CW laser excitation of stationary samples of NiTPP (nickel tetraphenylporphyrine) in pyridine and piperidine, using resonance Raman (RR) spectroscopy to monitor the ligation changes. The RR spectra also allow assessment of the structural change attendant upon ligation, and they permit identification of a 5-coordinate species in piperidine solution, with a ground state that is probably high spin.⁶ The same spinning vs. stationary sample technique was used which has allowed us to obtain triplet-state RR spectra of TPP complexes of Mg, Zn, and Pd.⁷

Figure 1 shows 406.7-nm-excited Raman spectra, in the region of the ν_4 skeletal mode,⁸ for a stationary sample of NiTPP in pyridine. Two ν_4 bands are seen, at 1369 and 1346 cm^{-1} . The former is at the frequency seen for NiTPP in noncoordinating solvents and is attributed to the low-spin 4-coordinate complex. The latter band is attributed to the 6-coordinate high-spin complex,

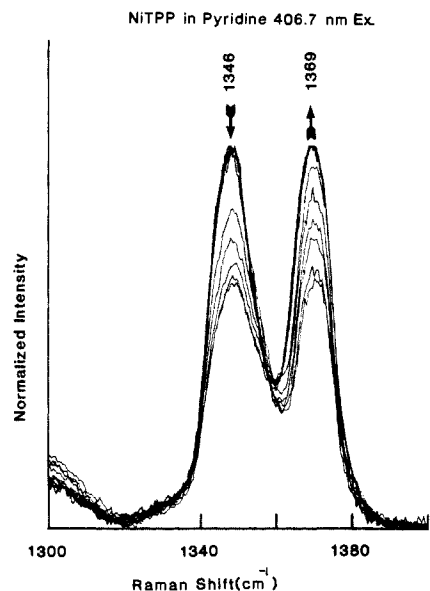


Figure 1. ν_4 Raman peaks for a stationary sample of NiTPP (purchased from Porphyrin Products and purified by chromatography on alumina A540, 0.2 mM) in pyridine, with 406.7-nm excitation. Arrows indicate the decreasing (1346 cm^{-1}) and increasing (1369 cm^{-1}) relative intensities at increasing laser power levels (1.5, 5, 10, 15, 20, 25, 50, 75, 90, 125, and 140 mW). In the absence of an internal standard (pyridine peaks are obscured by those of NiTPP) the spectra were scaled to whichever peak was stronger. (The intrinsic scattering factors are not the same for the two peaks.) Spectra were obtained via backscattering (135°) from a NMR sample tube, using a Spex 1401 double monochromator: 7- cm^{-1} slit width; 1-s time constant; 0.5 cm^{-1}/s scan rate.

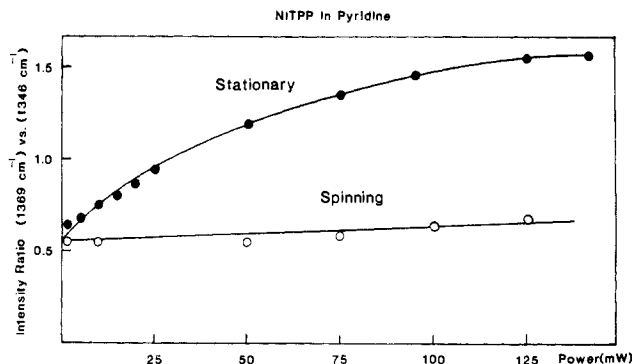


Figure 2. 1369/1346 cm^{-1} Raman peak height ratio for NiTPP in pyridine vs. 406.7-nm laser power for a stationary sample (\bullet) (see spectra in Figure 1) and a spinning sample (\circ).

by comparison with the spectrum of NiTPP in piperidine (see Figure 3) in which the 6-coordinate species is dominant.^{1,5} The porphyrin core is expanded in the 6-coordinate species due to electron promotion to the in-plane antibonding $d_{x^2-y^2}$ orbital; the porphyrin center-to-pyrrole nitrogen distance (C_1-N) is ~ 1.95 \AA in 4-coordinate nickel porphyrins,⁹ but 2.038 \AA in the bis-imidazole adduct of nickel tetramethylpyridylporphyrine.¹⁴ We attribute the ν_4 down shift upon pyridine or piperidine coordination at least in part to the core-size expansion; the porphyrin skeletal mode frequencies are known to be sensitive to the core size, as well as to electronic effects.¹⁵

* Author to whom correspondence should be addressed.

(1) (a) Kim, D.; Kirmaier, C.; Holten, D. *Chem. Phys.* **1983**, *75*, 305. (b) Kim, D.; Holten, D. *Chem. Phys. Lett.* **1983**, *98*, 584.

(2) (a) Kim, D.; Holten, D.; Gouterman, M. *J. Am. Chem. Soc.* **1984**, *106*, 2793. (b) Tait, C. D.; Holten, D.; Gouterman, M. *Chem. Phys. Lett.* **1983**, *100*, 268. (c) Tait, C. D.; Holten, D.; Gouterman, M. *J. Am. Chem. Soc.* **1984**, *106*, 6653.

(3) Martin, J. L.; Migus, A.; Poyart, C.; Lecarpentier, Y.; Astier, R.; Antonetti, A. *Proc. Natl. Acad. Sci. U.S.A.* **1983**, *80*, 173.

(4) (a) Gibson, Q. H.; Ainsworth, S. *Nature (London)* **1957**, *180*, 1416. (b) Hofrichter, J.; Sommer, J. H.; Henry, E. R.; Eaton, W. A. *Proc. Natl. Acad. Sci. U.S.A.* **1983**, *77*, 5608. (c) Frauenfelder, H.; Wolynes, P. G. *Science (Washington, D.C.)* **1985**, *229*, 337.

(5) Walker, F. A.; Hui, E.; Walker, J. M. *J. Am. Chem. Soc.* **1975**, *97*, 2390.

(6) Ake, R. L.; Gouterman, M. *Theor. Chim. Acta* **1970**, *17*, 408.

(7) Kim, D.; Terner, J.; Spiro, T. G. *J. Am. Chem. Soc.*, preceding paper in this issue.

(8) Stein, P.; Ulman, A.; Spiro, T. G. *J. Phys. Chem.* **1984**, *88*, 369.

(9) 1.929 \AA in tetragonal (D_{2d} , ruffled)¹⁰ and 1.958 \AA in triclinic (D_{4h} , planar)¹¹ nickel octaethylporphyrin; 1.960 \AA in nickel deuterioporphyrin;¹² 1.957 \AA in nickel etioporphyrin.¹³

(10) Meyer, E. F., Jr. *Acta Crystallogr., Sect. B* **1972**, *B28*, 2162.

(11) Cullen, D. L.; Meyer, E. F., Jr. *J. Am. Chem. Soc.* **1974**, *96*, 2095.

(12) Hamor, T. A.; Caughey, W. S.; Hoard, J. L. *J. Am. Chem. Soc.* **1965**, *87*, 2305.

(13) Fleischer, E. B. *J. Am. Chem. Soc.* **1963**, *85*, 146.

(14) Kirner, J. F.; Garofalo, J., Jr.; Scheidt, W. R. *Inorg. Nucl. Chem. Lett.* **1975**, *11*, 107.

(15) Spiro, T. G. In *Iron Porphyrins*; Lever, A. B. P., Gray, H. B., Eds.; Addison-Wesley: Reading, MA, 1983; Part Two, pp 89–159.